Available online at www.sciencedirect.com
SCIENCE DIRECT®
Journal of Nuclear Materials 343 (2005) 134–144
journal of nuclear materials
www.elsevier.com/locate/jnucmat

Fatigue properties of type 316LN stainless steel in air and mercury

J.P. Strizak [a,*], H. Tian [b], P.K. Liaw [b], L.K. Mansur [a]

[a] Metals and Ceramics Division, Oak Ridge National Laboratory, P.O. Box 2008, Oak Ridge, TN 37831-6088, USA
[b] Department of Materials Science and Engineering, The University of Tennessee, Knoxville, TN 37886-2200, USA

Abstract

An extensive fatigue testing program on 316LN stainless steel was recently carried out to support the design of the mercury target container for the spallation neutron source (SNS) that is currently under construction at the Oak Ridge National Laboratory in the United States. The major objective was to determine the effects of mercury on fatigue behavior. The *S–N* fatigue behavior of 316LN stainless steel is characterized by a family of bilinear fatigue curves which are dependent on frequency, environment, mean stress and cold work. Generally, fatigue life increases with decreasing stress and levels off in the high cycle region to an endurance limit below which the material will not fail. For fully reversed loading as well as tensile mean stress loading conditions mercury had no effect on endurance limit. However, at higher stresses a synergistic relationship between mercury and cyclic loading frequency was observed at low frequencies. As expected, fatigue life decreased with decreasing frequency, but the response was more pronounced in mercury compared with air. As a result of liquid metal embrittlement (LME), fracture surfaces of specimens tested in mercury showed widespread brittle intergranular cracking as opposed to typical transgranular cracking for specimens tested in air. For fully reversed loading (zero mean stress) the effect of mercury disappeared as frequency increased to 10 Hz. For mean stress conditions with *R*-ratios of 0.1 and 0.3, LME was still evident at 10 Hz, but at 700 Hz the effect of mercury had disappeared ($R = 0.1$). Further, for higher *R*-ratios (0.5 and 0.75) fatigue curves for 10 Hz showed no environmental effect. Finally, cold working (20%) increased tensile strength and hardness, and improved fatigue resistance. Fatigue behavior at 10 and 700 Hz was similar and no environmental effect was observed.

1. Introduction

The target material for the spallation neutron source (SNS) that is under construction at the Oak Ridge National Laboratory in the United States will be liquid mercury that is contained within a type 316LN SS vessel. The interaction of the energetic proton beam with the mercury target leads to high heating rates in the target. Although the resulting temperature rise is only about 10 °C, the rate of temperature rise is large ($\sim 10^7$ °C/s) during the beam pulse of ~0.7 μs, which occurs at a frequency of 60 Hz. The resulting thermal-shock induced compression of the mercury leads to the production of large amplitude high frequency pressure waves in the mercury that interact with the mercury target container and the bulk flow field. Temperature cycles due to beam trips and restarts also contribute to significant fatigue loads during operation.

* Corresponding author. Tel.: +1 865 574 5117; fax: +1 865 576 8424.
E-mail address: strizakjp@ornl.gov (J.P. Strizak).

0022-3115/$ - see front matter © 2005 Elsevier B.V. All rights reserved.
doi:10.1016/j.jnucmat.2005.03.019

In response to the need to provide test data and analysis for design and to ensure that the target module will meet its intended service, a materials research and development (R&D) program [1] has been carried out. One of the main components of the R&D program was a comprehensive fatigue testing program in both mercury and air under a wide range of conditions. A number of variables have been explored, including stress amplitude, cyclic frequency, minimum to maximum load ratio (R), and material condition.

2. Materials

Testing was performed on a single heat of mill-annealed type 316LN stainless steel purchased from Jessop Steel Company. Heat 18474 was melted by the electric-furnace, argon–oxygen decarburization process (EF/AOD) and met American Society of Mechanical Engineers (ASME) NCA3800 QSC-245 specification. Plate products consisting of 25 mm and 51 mm gauge plates met American Society for Testing and Materials (ASTM) A240-88c specification and were solution treated (annealed) at 1038 °C.

The composition of this low-carbon, nitrogen containing material is reported in Table 1. Metallography performed on the 25 and 51 mm plates revealed medium, uniform grain-size microstructures, and the measured ASTM grain size numbers were 3.7 and 3.2, respectively. Room temperature tensile properties for a strain rate of $8 \times 10^{-5}\ s^{-1}$ are given in Table 2. The observed modulus of elasticity was 197 GPa. Additional information on the microstructure and tensile properties of the 316LN stainless steel (heat 18474) can be found elsewhere [2].

Some of the mill-annealed plate was cold-worked to a level of 20% reduction in thickness. Table 3 gives the changes in tensile properties for 316LN stainless steel following the cold working treatment.

Table 1
Chemical composition of 316LN stainless steel (heat 18747) [wt%]

Element	Vendor (ladle)	ORNL (51 mm plate)	ORNL (25 mm plate)	ASTM specification	
				Min.	Max.
C	0.009	0.01	0.01		0.035
Mn	1.75	1.85	1.77		2
P	0.029	0.021			0.04
S	0.002	0.01			0.03
Si	0.39	0.51	0.47		0.75
Ni	10.2	10.3	9.77	10	14
Cr	16.31	16.5	15.1	16	18
Mo	2.07	2.09	1.97	2	3
Co	0.16	0.14	0.17		
Cu	0.23	0.26	0.23		
N	0.11	0.13	0.12	0.1	0.16
Fe	Bal.	Bal.	Bal.	Bal.	Bal.

Table 2
Room temperature tensile properties for 316LN stainless steel (heat 18474) for a strain rate of $8 \times 10^{-5}\ s^{-1}$

0.2% Offset yield strength	259.1 Mpa
Ultimate strength	587.5 Mpa
Elongation	86.20%
Reduction in area	88.11%
Vickers hardness	203.5

3. Experimental

3.1. Equipment and test methods

Constant amplitude, uniaxial fatigue testing was conducted on commercially available servo-hydraulic testing machines incorporating basic components including a hydraulic power supply, state-of-the-art digital feedback control instrumentation, and a mechanical load frame equipped with a force (load) measurement transducer, a servo-valve/hydraulic actuator assembly, and test specimen gripping fixtures. In addition, specialized fixtures were required for in situ exposure of the test specimen to liquid mercury. Further, during high frequency testing self-heating, caused by mechanical working of the specimen, required supplemental cooling to keep the specimen temperature below 100 °C.

Load-control fatigue tests under fully-reversed, and positive tensile mean stress were conducted in air and in mercury. Cyclic loading waveform frequency ranged from 0.1 to 700 Hz. The fatigue testing program described in this report was a collaborative effort between Oak Ridge National Laboratory (ORNL) and the University of Tennessee (UT). Testing at ORNL was limited to a maximum of 10 Hz whereas high frequency capability was provided by UT. A sinusoidal waveform was employed for load-control testing.

Fully reversed strain-control testing was performed in air only. Whereas the purpose of the load-control tests was to determine the effects of mercury, the main purpose of the strain-control tests was for comparison of our material with ASME data on generic type 316 stainless steel. An axial-displacement extensometer, mounted directly to the specimen gage section, was employed in controlling the cyclic strain applied to the specimen. The cyclic strain waveform was triangular, and the frequency, limited by the response characteristics of the extensometer, was less than 1 Hz. Testing over the range of cyclic lifetimes was conducted at a constant strain rate of $4 \times 10^{-3}\ s^{-1}$.

Load-control and strain-control fatigue testing with fatigue lifetimes less than 10^5 cycles were conducted in

Table 3
Room temperature tensile properties for annealed and cold-worked 316LN stainless steel (heat 18474) for a strain rate of $8 \times 10^{-5}\ s^{-1}$

Material condition	0.2% Offset yield strength (MPa)	Ultimate strength (MPa)	Elongation (%)	Reduction of area (%)	Vickers hardness
Mill-annealed	259.1	587.5	86.20	88.11	203.5
20% Cold work	733.4	800.0	9.72	81.88	274.2

accordance with ASTM Standard E606, 'Standard Recommended Practice for Constant-Amplitude Low-cycle Fatigue Testing' [3]. High cycle fatigue tests were conducted in accordance with ASTM Standard E466, 'Standard Practice for Conducting Constant Amplitude Axial Fatigue Tests of Metallic Materials' [4]. These standards make specific references to other appropriate standards which address such factors as load and extensometer calibration, alignment of specimen gripping fixtures, and specimen design and preparation.

3.2. Fatigue specimens

Fatigue specimens were machined such that the longitudinal axis of the specimen was parallel to the primary rolling direction of the 316LN stainless steel plate material. Four specimen designs were used depending on the fixtures available on a particular testing machine. Schematic drawings of the specimen designs are shown in Figs. 1 and 2. Each specimen design features a central, uniform-gage test section. The diameter, d, of the gage section ranged from 5.08 mm to 7.62 mm and, in accordance with ASTM E606 recommendations, the length of the gage section was $2d$ to $4d$. In order to provide consistent test results from the different specimen designs, particular attention was given to surface preparation in the gage section using the same procedure for each of the four specimen designs. In the final stages of machining 0.250 mm of material was removed by low stress grinding, and the remaining 0.025 mm of excess material in the gage section was removed by longitudinal polishing to remove any radial machining marks and to produce maximum surface roughness to 0.2 μm.

Tight geometric feature tolerances (concentricity, parallelism, and perpendicularity) specified for specimen machining, and precise alignment of the specimen gripping fixtures (ASTM Standard E1012, 'Standard Practice for Verification of Specimen Alignment Under Tensile Loading' [5]) resulted in highly accurate loading of the specimen along its longitudinal axis with minimal bending strains, well within the limits allowed by ASTM standard practices E466 and E606.

3.3. Fixtures for testing in mercury

The ORNL fatigue specimen (5.08 mm diameter gage section) for load-control tests in air and mercury is shown in Fig. 1. To hold mercury around the gage section of the specimen for in situ tests, a vial was machined from commercially pure nickel and press-fit to each specimen. The assembly (Fig. 3) was then ultrasonically cleaned and filled with mercury prior to mounting in the specimen grips. A bushing of nickel was added to the top

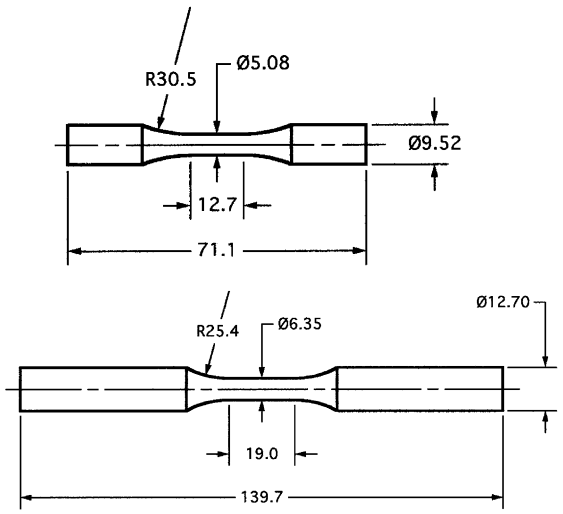

Fig. 1. ORNL fatigue specimens. Dimensions in millimeters.

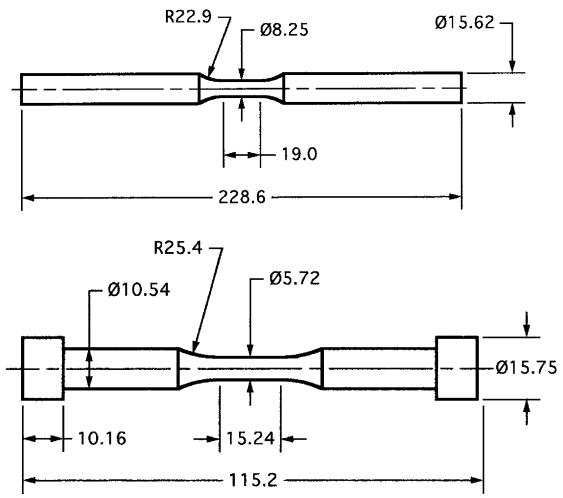

Fig. 2. UT fatigue specimens. Dimensions in millimeters.

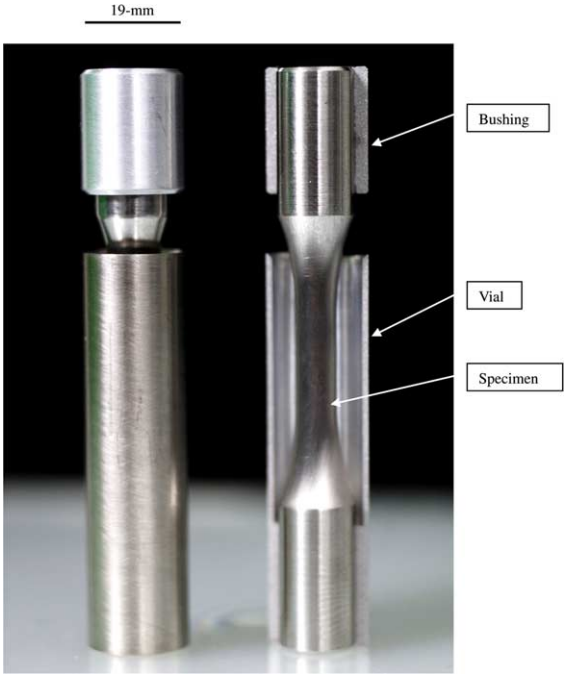

Fig. 3. ORNL fatigue specimen with bushing and vial for containment of mercury.

of the specimen to provide the same diameter for top and bottom grips.

At the University of Tennessee, a reusable, 3-piece container machined from 304 stainless steel, was employed for each of the two specimen sizes (Fig. 2). A tubular container was threaded onto a split collet with a smooth bore to accommodate the shank diameter of the specimen. The assembly was held in place on the shank of the specimen using a silicone-rubber adhesive sealant. Fig. 4 shows the container mounted to a button end specimen. Similarly, an appropriately sized container was fabricated for the large straight-shanked specimen (Fig. 2).

3.4. Supplemental cooling

Initial experience at UT in high frequency testing at 700 Hz under tensile mean stress loading conditions in air showed that the test specimen temperature would rise by several hundred degrees celsius. The temperature increased as the applied maximum stress of the loading cycle increased. The observed self-heating of the specimen was caused by inelastic effects including plastic deformation and internal friction [6]. On the other hand, in mercury the rise in temperature did not exceed 78 °C since mercury acts as a coolant.

Generally, significant increases in temperature are known to decrease fatigue life. Therefore, a supplemental cooling apparatus was fabricated. Cold nitrogen gas,

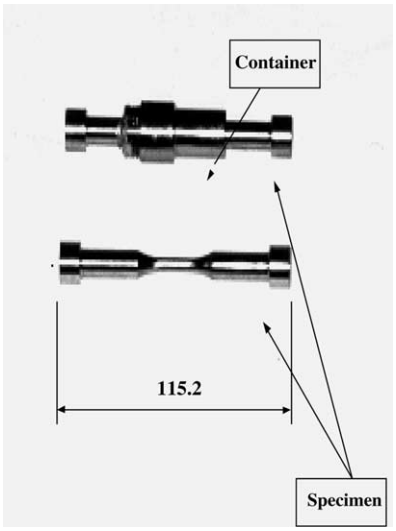

Fig. 4. Mercury container mounted to a UT button-end fatigue specimen.

cooled by passing the gas through a dewar containing liquid nitrogen, was continuously flowed over the surface of the specimen. Thermocouples were used to monitor the outlet temperature of the nitrogen gas and the specimen gage section, while the flow rate of the nitrogen gas was controlled manually. Additional information can be found elsewhere [7].

Significant self-heating of the specimen was also observed in fully reversed load-control testing in air at 10 Hz. Further, specimen temperatures in mercury also exceeded 100 °C. To provide cooling for specimens tested in mercury, copper tubing was simply wound around the outer surface of the mercury container and once through chilled water provided adequate cooling of the mercury and the test specimen. For specimens tested in air, cooled nitrogen gas was used, as for the 700 Hz tests.

4. Results and discussion

4.1. Strain-control tests

Strain-control fatigue testing of 316LN stainless steel in air was intended to be largely confirmatory to compare the data with the historical data base on other 300-series austenitic stainless steels which provided the basis for establishing the ASME Code Sect. III design curve [8]. Results of fully reversed (tension–compression) room temperature strain-control tests are given in Fig. 5. Uniform-gage specimens with 5.08 mm and 6.35 mm diameter gage sections (Fig. 1) were tested in air employing a triangular waveform providing a

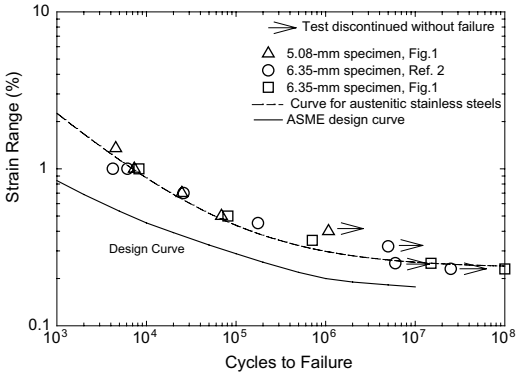

Fig. 5. Strain-control fatigue test results.

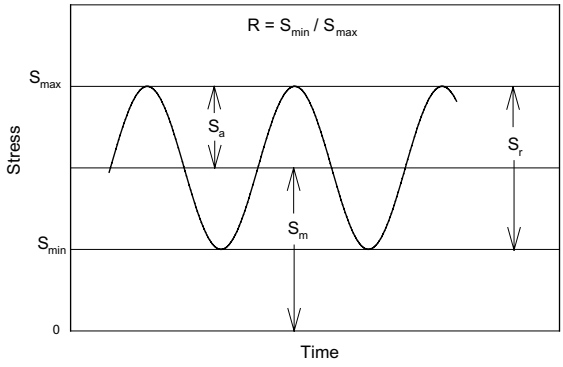

Fig. 6. Applied stress parameters for load-control fatigue.

constant strain rate of 10^{-3} s^{-1}. No effect of specimen size was observed.

Fig. 5 includes a mean curve for austenitic stainless steels. This curve became the basis for establishing the ASME design curve. The historical data were modeled using a power law relationship in terms of stress amplitude, S_a (GPa), and cycles to failure, N:

$$S_a = 62.4N^{-0.5} + 0.228. \quad (1)$$

Stress amplitude for the strain-control data was defined as

$$S_a = 0.5M\varepsilon_t, \quad (2)$$

where ε_t is the total strain range, and M is the modulus of elasticity (195 GPa). The 316LN data in Fig. 5 are in good agreement with the curve for austenitic stainless steels.

The ASME Code constructed a design curve by dividing the fatigue life for a given stress amplitude (Eq. (1)) by 20. In order to present the design curve in terms of strain range (Fig. 5), stress amplitude was converted to strain range (%) using:

$$\varepsilon_t = 2S_a/M * 100. \quad (3)$$

Fig. 5 confirms that the ASME design curve is applicable to type 316LN stainless steel.

4.2. Load control tests

The applied stresses in uniaxial, constant amplitude load-control fatigue testing are described by three parameters. The nomenclature used to describe the test parameters in cyclic-stress testing are shown in Fig. 6. The mean stress, S_m is the arithmetic average of the maximum stress, S_{max}, and the minimum stress, S_{min}, in a cycle, i.e., $S_m = (S_{max} + S_{min})/2$. The stress range, S_r is the arithmetic difference between the maximum and minimum stresses, or $S_r = S_{max} - S_{min}$. And the stress amplitude, S_a, also referred to as the alternating stress, is one half of the stress range, $S_a = S_r/2 = (S_{max} - S_{min})/2$.

In fully reversed, tension–compression load cycling, the mean stress, S_m, is zero, and the familiar ratio of minimum to maximum stress, $R = S_{min}/S_{max}$ is -1. If the load is cycled between a tensile maximum and no load, the stress ratio, R, becomes zero and the mean stress, S_m is one half the maximum stress, $S_{max}/2$. And if the stress is cycled between two tensile stresses, the stress ratio, R becomes a positive number greater than zero but less than 1, and the mean stress can be expressed as $S_m = (1 + R)S_{max}/2$.

For the present study, testing was limited to fully reversed loading with $R = -1$, and tension–tension loading with mean stress conditions described by $R = 0.1$, 0.3, 0.5, and 0.75. The tests results are presented herein using the familiar S–N fatigue curve format with alternating stress, S_a (linear scaling) plotted as a function of cycles to failure, N (logarithmic scaling).

Results of fully reversed, tension–compression room temperature fatigue tests ($R = -1$) for annealed 316LN stainless steel are shown in Fig. 7. Generally, fatigue life

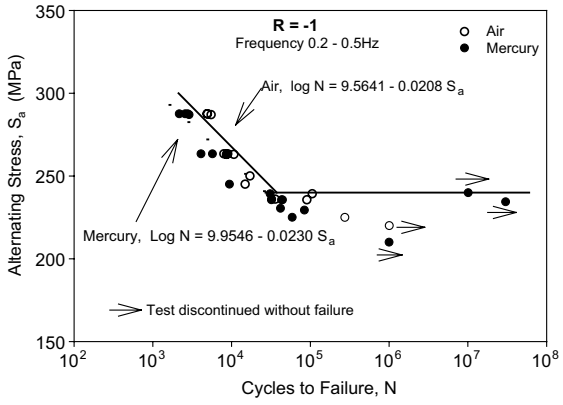

Fig. 7. Curve fits for $R = -1$ in air and mercury at frequencies in the range 0.2–0.5 Hz.

increases as stress amplitude decreases, and data at low stresses leveled off becoming horizontal, defining a limiting stress. Below this limiting stress, known as the fatigue limit or endurance limit, the material did not fail. At high stresses, mercury appeared to reduce fatigue life by a factor of 2–3 while the endurance limit appeared to be converging at approximately 240 MPa.

The *S–N* relationships in air and mercury are reasonably approximated by two linear segments on semilogarithmic coordinates. In each of the *S–N* plots, the horizontal line, which was determined visually, represents the endurance limit for the given *R*-ratio in either air or mercury. For stresses above the endurance limit the data were statistically fitted according to ASTM standard E739 [9], 'Standard Practice for Statistical Analysis of Linear or Linearized Stress–Life (*S–N*) and Strain–Life (*ε–N*) Fatigue Data'. The linearized relationship employed was

$$\mathrm{Log}N = A + BS_a. \tag{4}$$

The following discussion address the effects of *R*-ratio (mean stress), test frequency, and mercury on the fatigue behavior of 316LN stainless steel.

4.2.1. Frequency effects in air and mercury

The effect of frequency on the fatigue behavior of materials has been studied by other workers under various test conditions. Investigations have been conducted at low frequencies (<5 Hz), high frequencies (5–1000 Hz), and in the ultrasonic range (20 kHz). Increasing test frequency has been reported to either increase or decrease lifetimes, as well as to have negligible effects on the fatigue life of a material [10–15].

A study of the influence of frequency on the cyclic crack propagation rate of AISI type 304 stainless steel showed that the crack propagation rate increased with a decrease in frequency below 5 Hz. Fatigue crack propagation tests conducted on the powder-metallurgy, nickel-based superalloy KM4 at room temperature indicated no effect of frequency on the fatigue behavior at room temperature [15]. In fatigue crack growth tests on 316 stainless steel in air at 538 °C, it has been observed that at frequencies in the range of 0.0067–6.67 Hz, crack growth rate increased as the frequency decreased.

In the present work considerable number of load-control fatigue tests were conducted on 316LN stainless with $R = 0.1$ over a frequency range of 10–0.1 Hz in air and mercury as shown in Fig. 8. Fitted *S–N* curves for air and mercury are given in Figs. 9 and 10, respectively, derived from the data of Fig. 8. In air data at 1.0 Hz showed a 30–50% reduction in fatigue lifetimes compared with results at 10 Hz. The endurance limit remained unchanged. Limited testing at 0.1 Hz suggest that no further reduction in fatigue life would be expected at frequencies less than 1.0 Hz.

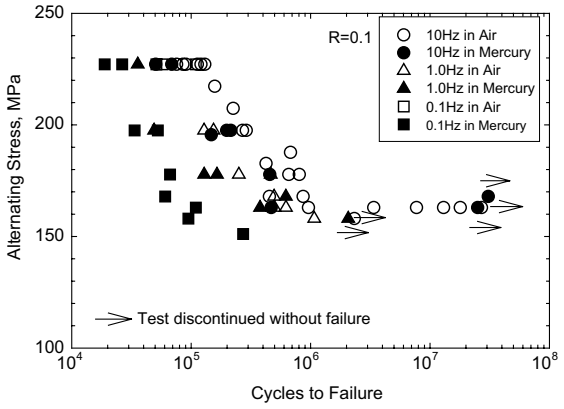

Fig. 8. Fatigue test results for $R = 0.1$.

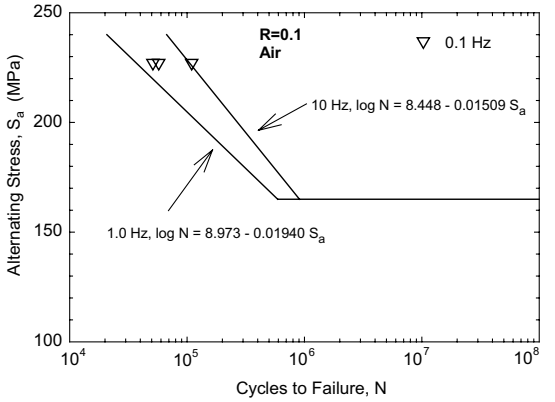

Fig. 9. *S–N* fatigue curves for $R = 0.1$ in air at room temfperature.

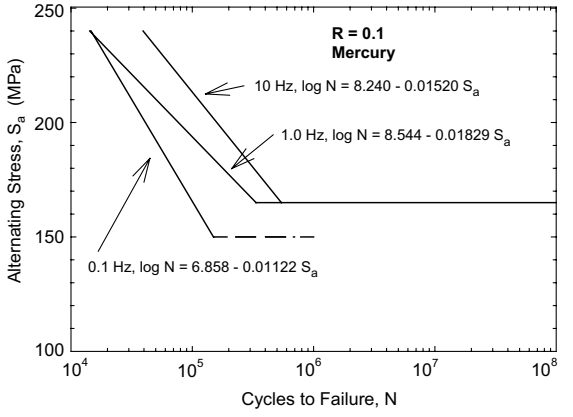

Fig. 10. *S–N* fatigue curves for $R = 0.1$ in mercury at room temperature.

Reviewing Figs. 9 and 10, the effect of frequency appears to be more pronounced in mercury compared with

tests in air. This suggests that there is a synergistic relationship between frequency and environment.

4.2.2. Effects of mercury

Liquid metal embrittlement (LME) has mainly been examined by means of standard tensile tests or slow strain-rate tests [16–19], rather than by cyclic loading tests (fatigue).

Mercury is known to embrittle aluminum, brass, and some nickel-base alloys [20]. Room temperature tensile properties may remain the same, but fractures in mercury may be less ductile, exhibiting varying degrees of intergranular cracking. In slow strain rate tests the time to failure can be significantly reduced in mercury.

Little information on LME in stainless steels was found. Krupowicz [21] indicated that types 304 and 304L stainless steels were somewhat embrittled in mercury in slow strain rate tests at room temperature, but types 316 and 316L were not.

At the beginning of the SNS Research and Development program for target materials, constant extension rate tensile tests of 316 stainless steel were conducted in air and mercury [22]. One set of specimens was tested in the mill annealed condition; another was heat treated to produce a microstructure sensitive to stress corrosion cracking; and a third was autogenously welded using the gas–tungsten arc process. These tests did not reveal any effect of mercury (compared to air) on the tensile properties in any of the three heat treat conditions. It was noted, however, that the fresh fracture surface of specimens tested in mercury was invariably wetted by the mercury while the rest of the specimen surface was not. Although the phenomenon of LME has been known for over a hundred years, it is still not well understood [23]. However, for LME to occur a metal subjected to an applied tensile stress must be wetted by the liquid. Without wetting, LME is unlikely.

Our screening tests [24] involving load-control fatigue of 316LN stainless steel at $R = -1$, similarly reported that post-test fracture surfaces were completely wetted by mercury and that fatigue lives were decreased in mercury compared with air. In fatigue, cracks typically initiate in one or more locations on the surface of the specimen. When cracks open in the presence of air, the crack faces quickly develop a protective oxide and propagation of the crack depends on the state of stress and physical characteristics of the bulk material. However, when fatigue cracks open in a mercury environment, the fresh fracture surfaces are wetted by the mercury. Crack propagation then depends upon the interaction of the mercury with the material (particularly grain boundaries) in addition to the bulk properties of the material.

Generally, when investigating environmental effects on fatigue, stress amplitude is not the only factor affecting material/environment interaction. Time dependent effects can also be of importance. When failure occurs by environmental fatigue, stress-cycle frequency, stress-waveshape, and mean stress can synergistically affect the cracking process. The frequency dependence of environmental fatigue is generally thought to result from the fact that interaction of a material and its environment is essentially a rate-controlled process. Low cycle-frequencies, when there is substantial elapsed time between changes in stress levels, allow more time for interaction between material and environment than do higher frequencies. Also, when environments have a deleterious effect on fatigue behavior, a critical range of frequencies of loading may exist in which mechanical/environmental interaction is significant. Above this range the effect may diminish or disappear.

Comparing Figs. 9 and 10, lifetimes in mercury at 10 Hz were less than those observed in air by approximately a factor of 2 at stress levels above the apparent fatigue limit. Further, when the test frequency was lowered to 0.1 Hz, the resultant reduction in fatigue life in mercury was significantly greater than observed in air. Fatigue lifetimes in mercury at 0.1 Hz were found to be approximately 70% lower than those at 10 Hz in mercury and nearly an order of magnitude lower than the results in air at 10 Hz. The data also suggest that at the lowest frequency (0.1 Hz) mercury may even reduce the fatigue limit. Since wetting is essential, LME by mercury has no likely effect on crack initiation, but mercury apparently enhances crack propagation rates, and consequently lowers fatigue life. Evidence of LME was also observed in SEM examinations of the fracture surfaces of fatigue specimens tested at $R = -1$ and $R = 0.1$ at stress amplitudes above the endurance limit. For example, Fig. 11 shows micrographs of the typical crack propagation regions for specimens tested at $R = 0.1$ in air and mercury. The specimen tested in air showed transgranular cracking across most of the fracture surface. In contrast, the specimen tested in mercury exhibited a more brittle appearance with wide spread intergranular cracking.

Fig. 12 compares fatigue lives in air and mercury at a cyclic loading frequency of 700 Hz. At 10 Hz fatigues lives in mercury at stress amplitudes above the endurance limit were less than in air by a factor of two. But it appears that between 10 Hz and 700 Hz the deleterious effect of mercury has disappeared.

Over the frequency range of 0.1–700 Hz the endurance limit for $R = 0.1$ was unaffected by either frequency or environment. However, mean stress (R-ratio) was observed to affect the fatigue behavior of 316LN stainless steel.

4.2.3. Mean stress effects

Tensile mean stress is known to enhance fatigue crack initiation and increase stable crack propagation rates in steels [25]. Fig. 13 shows the family of 316LN

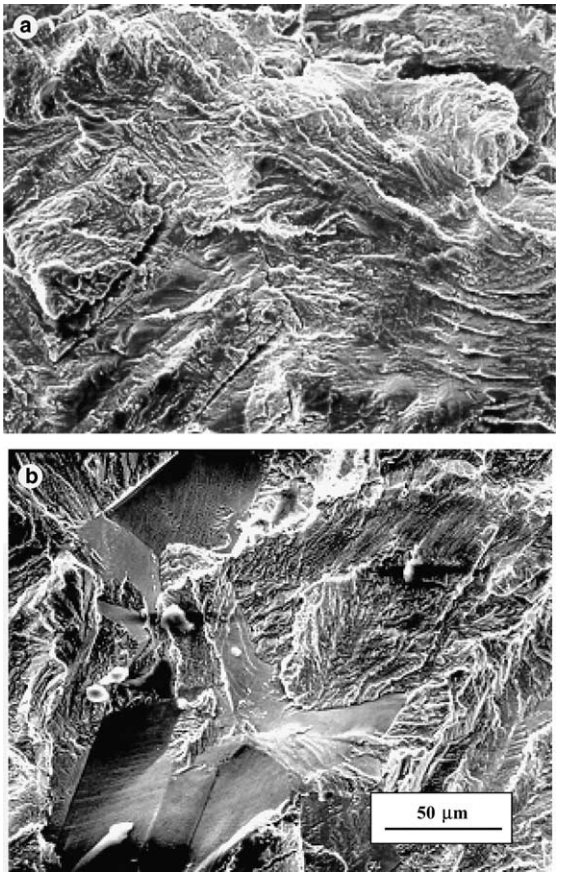

Fig. 11. Fracture surface showing the typical fracture modes in the crack-propagation areas for specimens was at 10 Hz with a stress amplitude of 208 MPa and $R = 0.1$: (a) transgranular cracking in air; (b) intergranular cracking in mercury.

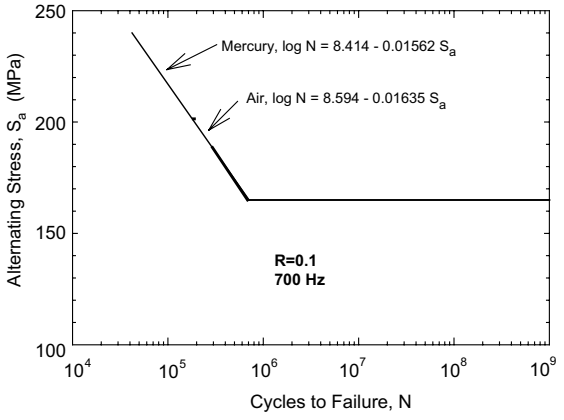

Fig. 12. *S–N* fatigue curves for $R = 0.1$ at 700 Hz. Specimen self-heating was encountered in air. Supplemental cooling kept specimen temperatures <100 °C.

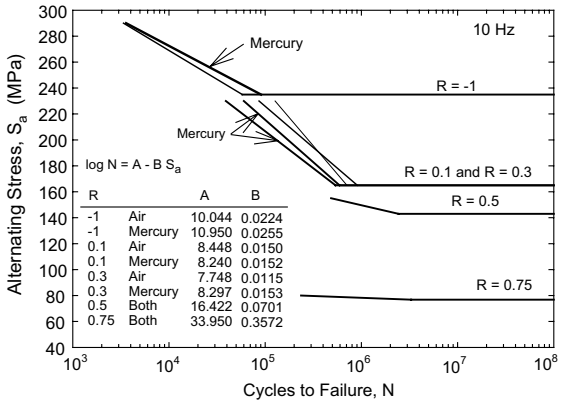

Fig. 13. *S–N* curves for various mean stress conditions.

stainless steel *S–N* fatigue curves (developed under the subject test program) at a cyclic loading frequency of 10 Hz for zero mean stress ($R = -1$) and a number of tensile mean stress conditions with $R = 0.1$ to 0.75. At $R = -1$ the endurance limit for air and mercury is around 240 MPa. Additionally, the effect of mercury observed at lower frequencies (Fig. 7) has disappeared. Increasing mean stress decreases the fatigue resistance of the material. A tensile mean stress condition of $R = 0.1$ decreased the fatigue limit (in air and mercury) to around 170 MPa. At stresses above the endurance limit, the degrading effect of mercury is still evident. However, the environmental effect disappears at higher frequencies (Fig. 12). The endurance limit remains unaffected as *R*-ratio is increased to 0.3, and the effect of mercury is still evident at higher stress levels. Upon further increases in mean stress the endurance limit again decreases to around 140 MPa and around 77 MPa for $R = 0.5$ and 0.75, respectively. But for $R = 0.5$ and $R = 0.75$ there is apparently no effect of mercury over the entire range of fatigue life investigated.

For design purposes it is useful to know how mean stress affects the allowable alternating stress amplitude for a given fatigue life requirement. (Alternating stress, S_a, and mean stress, S_m, are defined at the beginning of Section 4.2 and are shown schematically in Fig. 6.) At zero mean stress (fully reversed, tension–compression loading), the allowable stress amplitude is the fatigue strength for a specific fatigue life. As the mean stress increases, the permissible amplitude decreases in order to achieve the same fatigue life. And at a mean stress equal to the ultimate tensile strength of the material, the allowable cyclic amplitude is zero. Mean stress data are generally presented in terms of constant life diagrams that plot all combinations of alternating stress and mean stress resulting in the same specified life to failure.

Two of the most widely used empirical relationships for describing the effect of mean stress on fatigue life,

i.e., the modified Goodman relation and the Gerber parabola, [26] are shown in Fig. 14. The straight line joining the fully reversed (zero mean stress) alternating fatigue strength for a given fatigue life to the ultimate tensile strength, S_u, of the material is the modified Goodman relation which is as a rule-of-thumb, applicable to brittle materials but conservative for ductile materials. Gerber's relation provides a parabolic relationship between S_a and S_u which is generally applicable to ductile materials. The relations are written as

Modified Goodman relation:

$$S_a = S[1 - (S_m/S_u)] \tag{5}$$

and

$$\text{Gerber's relation}: \; S_a = S[1 - (S_m/S_u)^2], \tag{6}$$

where S_a is the alternating stress associated with a mean stress, S_m, S is the alternating fatigue strength (with zero mean stress) resulting in the specific fatigue life of interest, and S_u is the ultimate tensile strength of the material.

For fully reversed, zero mean stress, $R = -1$ cyclic loading, the S–N data in Fig. 13 level off around 10^5 cycles indicating a fatigue endurance limit in either air or mercury around 240 MPa, the alternating stress amplitude below which fatigue failure will not occur. This value along with the reported ultimate tensile strength of the type 316LN stainless steel was used to construct the constant-life diagram for 10^6 cycles given in Fig. 14, used here to show the effect of mean stress on the endurance limit for the 316LN material.

When the loading cycle incorporates a tensile mean stress described by $R = 0.1$, the observed endurance limit (see Fig. 13) is reduced to 170 MPa. The experimental observation lies near the modified Goodman prediction shown in Fig. 14. Though the mean stress is higher, the alternating stress for $R = 0.3$ (Fig. 14) is the same as for the $R = 0.1$ condition. This experimental observation is higher than predicted by the modified Goodman line, but lies near the Gerber parabola. For $R = 0.5$ and 0.75 the endurance limits decreased with the increasing mean stress as expected, but, in both cases, the experimentally determined alternating stresses were higher than predicted by either the modified Goodman line or the Gerber parabola (Fig. 14). Both relationships yielded conservative estimates of the allowable alternating stress to maintain the specified cyclic life. Still, these empirical relationships can be a useful tool for initial estimates of the allowable alternating stress for a given mean stress condition when cyclic life is specified.

4.3. Load-control tests on cold-worked material

Room temperature load-control tests on 20% cold worked 316LN stainless steel were conducted in air and mercury with an R-ratio of 0.1 at test frequencies of 10 and 700 Hz.

Generally, the fatigue strength of a metal or alloy increases with increasing yield and ultimate tensile strengths. Table 3 gives the changes in tensile properties for 316LN stainless steel following cold working. For a 20% cold working treatment the yield and ultimate tensile strengths were increased by factors of approximately 3 and 1.5, respectively. As shown in Fig. 15 fatigue resistance was improved significantly.

Fatigue lives in air for the cold-worked material at 10 and 700 Hz are comparable. Further, lifetimes in air and mercury are comparable. However, there is a noticeable change in the shape of the S–N curves compared to the annealed material. Fatigue curves for annealed 316LN stainless steel exhibit a sharp knee in the S–N curve at approximately 1-million cycles (e.g. Figs. 9 and 10). Fatigue life increases as stress amplitude decreases and then levels off defining a fatigue limit. The S–N curve is reasonably described by a bilinear relationship (Fig. 15). On the other hand, the S–N relationship for the cold-worked material is much flatter (Fig. 15) and a single

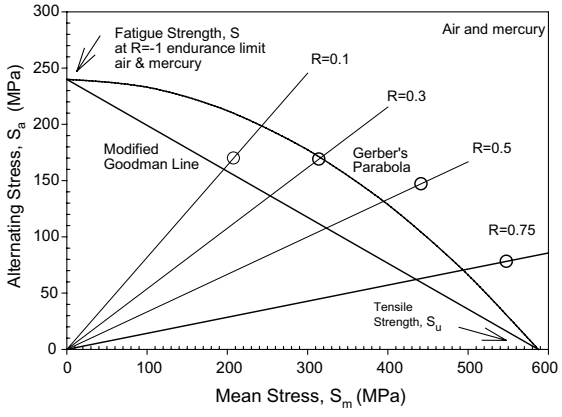

Fig. 14. Constant life diagram for a fatigue life of 10^6 cycles.

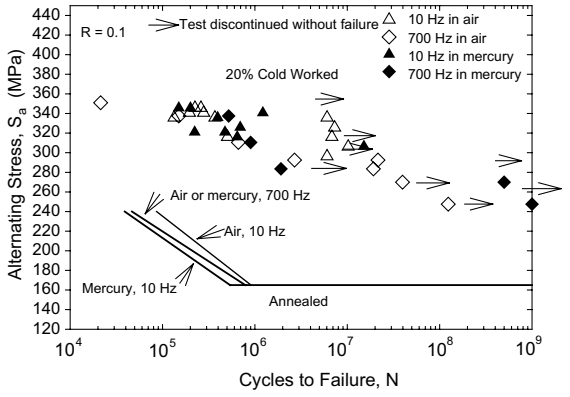

Fig. 15. S–N fatigue of cold-worked 316LN stainless steel.

linear relationship may be appropriate for estimating fatigue lives.

Cold working is also known to improve fatigue fracture resistance. Fatigue crack growth rates of austenitic stainless steels have been studied extensively given their wide spread use in high temperature structural applications. Cold working is one of the strengthening mechanisms used for improving the strength of 304 and 316 stainless steels. Cold working (20–25%) has been shown [27] to reduce crack growth rates at room and elevated temperatures.

In addition to the subject fatigue test program, another major activity in the materials research and development program for the SNS target module is an investigation of cavitation erosion (pitting) of the structural material caused by the proton-pulse induced pressure wave [2]. In general the greatest resistance to pitting is shown by those alloys that offer a combination of high strength, hardness, and toughness. The resistance of a material to pitting can be improved by: (1) a surface hardening treatment such as carburizing or shot peening, (2) a surface coating treatment such as spraying, cladding or plating, or (3) increasing the bulk strength and hardness by heat treating or cold working. Cavitation erosion testing in mercury is comparing annealed 316LN stainless steel with 316LN in other conditions, one of which is cold working. Results from the fatigue testing program showing higher fatigue strength following cold working with no observed effect of mercury on fatigue life will be taken into consideration when evaluating potential target vessel design modifications related to cavitation.

A third activity in the SNS materials research and development program is in the area of radiation-induced changes in properties. Determining tensile and fatigue properties of specimens dynamically under irradiation and in contact with mercury would be very challenging and likely cost prohibitive. Based on the widely known similarities of irradiation and cold-working for producing both increases in dislocation density and increases in yield stress, and in the absence of capabilities to test irradiated materials in fatigue, the fatigue testing program included cold-worked material. Tensile properties have been obtained on a number of irradiated (not in mercury) austenitic stainless steels including annealed 316LN [28]. In general, yield and ultimate tensile strengths increased with increasing fluence while ductility (elongation) decreased. Available data on the effects of cold working on the tensile properties of type 316 stainless steel show similar changes in strength and ductility with increasing levels of cold work [29]. Farrell [30] has observed that a 20% cold working treatment induces properties that closely match those produced by an irradiation dose of about 1 dpa at irradiation temperatures below 100 °C. However, it should also be pointed out that there are significant differences in the dislocation microstructures (and other microstructural features) between irradiated material and unirradiated material that is cold worked. Given that there appears to be a correlation between the tensile and fatigue strengths of 316LN stainless steel, fatigue data on cold-worked material may provide some insight on the effects of irradiation on fatigue behavior.

5. Conclusions

The *S–N* fatigue behavior of 316LN stainless steel is characterized by a family of bilinear fatigue curves, which are dependent on frequency, environment, mean stress and cold work. Generally, fatigue life increases with decreasing stress and levels off in the high cycle region to an endurance limit below which the material did not fail. For fully reversed loading as well tensile mean stress loading conditions, mercury had no effect on endurance limit. However a synergistic relationship between mercury and cyclic loading frequency was observed at low frequencies. As expected, fatigue life decreased with decreasing frequency, but the response was more pronounced in mercury compared with air. As a result of LME, fracture surfaces of specimens tested in mercury showed widespread brittle intergranular cracking as opposed to typical transgranular cracking for specimens tested in air. For fully reversed loading (zero mean stress) the effect of mercury disappeared as frequency increased to 10 Hz. For mean stress conditions with *R*-ratios of 0.1 and 0.3 LME was still evident at 10 Hz, but at 700 Hz the effect of mercury had disappeared ($R = 0.1$). Further, for higher *R*-ratios (0.5 and 0.75) fatigue curves for 10 Hz showed no environmental effect. Finally, cold working (20%) increased tensile strength and hardness, and improved fatigue resistance. Complete documentation on the fatigue program can be found in Ref. [31].

Acknowledgment

Research was sponsored by the Office of Science, US Department of Energy, under contract no. DE-AC05-00OR22725 with UT-Battelle, LLC.

References

[1] L.K. Mansur, T.A. Gabriel, J.R. Haines, D.C. Lousteau, J. Nucl. Mater. 296 (2001) 1.
[2] R.W. Swindeman, HWR-NPR Materials/Systems Integrity Mechanical Behavior Report, ORNL/NPR-92/94, Martin-Marietta Energy Systems, Incorporated, Oak Ridge National Laboratory, June 1993.
[3] Annual Book of ASTM Standards, vol. 03.01, E606-80, 1992.

[4] Annual Book of ASTM Standards, vol. 03.01, E466-82, 1992.
[5] Annual Book of ASTM Standards, vol. 03.01, E1012-89, 1992.
[6] P.K. Liaw, H. Wang, L. Jaing, J.Y. Huang, R.C. Kuo, J.G. Huang, Scr. Mater. 42 (2000) 389.
[7] H. Tian, P.K. Liaw, J.P. Strizak, L.K. Mansur, J. Nucl. Mater. 318 (2003) 15.
[8] Boiler and Pressure Vessel Code, Section III, Division 1, Subsection NB Class 1 Component, American Society of Mechanical Engineers, New York, 1 July 1998.
[9] Annual Book of ASTM Standards, vol. 03.01, E739-91, 1992.
[10] A. Plumtree, S. Schafer, ASTM STP 942, ASTM, Philadelphia, PA, 1988, p. 2249.
[11] J.Y. Guinemer, A. Plumtree, ASTM STP 765, ASTM, Philidelphia, PA, 1982, p. 452.
[12] T. Yokobori, K. Sato, Eng. Fract. Mech. 8 (1976) 81.
[13] B. Mukherjee, D.J. Burns, Exp. Mech. 11 (1971) 433.
[14] K. Sadananda, P. Shaninian, Metall. Trans. A 11 (1980) 267.
[15] S.A. Padula II, A. Shyam, R.O. Ritchie, W.W. Milligan, Int. J. Fatigue 21 (1999) 725.
[16] C.E. Price, J.K. Good, Trans. Am. Soc. Mech. Eng. (ASME) 106 (1984) 178.
[17] J.J. Krupowicz, J. Eng. Technol. 111 (1989) 229.
[18] C.E. Price, L.B. Taylor, Natl. Assoc. Corros. Eng. 43 (1987) 229.
[19] D.A. Wheeler, R.G. Hoagland, J.P. Hirth, Corrosion 45 (1989) 207.
[20] C.E. Price, J.K. Good, ASME J. Eng. Mater. Technol. 106 (1984) 184.
[21] J.J. Krupowicz, in: R.D. Cane (Ed.), Slow Strain Rate Testing for the Evaluation of Environmentally Induced Cracking: Research and Engineering Applications, ASTM STP 1210, ASTM, Philadelphia, 1993, p. 193.
[22] J.R. DiStefano, S.J. Pawel, E.T. Manneschmidt, Materials Compatibility Studies for the Spallation Neutron Source, ORNL/TM-13675, September, 1998.
[23] V.I. Igoshev, L.G. Rogova, L.I. Trusov, T.P. Khvostantseva, J. Mater. Sci. 29 (1994) 1569.
[24] S.J. Pawel, J.R. DiStefano, J.P. Strizak, C.O. Stevens, E.T. Manneschmidt, Screening Test Results of the Fatigue Properties of Type 326LN Stainless Steel in Mercury, ORNL/TM-13759, SNS/TSR-0097, March, 1999.
[25] ASM Handbook Fatigue and fracture, vol. 19, ASM International, Metals Park, OH, 1996, p. 639.
[26] ASM Handbook Mechanical testing, vol. 8, ASM International, Metals Park, OH, 1989, p. 374.
[27] ASM Handbook Fatigue and fracture, vol. 19, ASM International, Metals Park, OH, 1996, p. 605.
[28] K. Farrell, T.S. Byun, J. Nucl. Mater. 296 (2001) 129.
[29] Chromium–nickel Stainless Steel Data, 3rd Ed., The International Nickel Company, New York, 1970, p. 23.
[30] K. Farrell, Oak Ridge National Laboratory, letter to J.P. Strizak, 29 August 2002.
[31] J.P Strizak, H. Tian, P.K. Liaw, L.K. Mansur, Fatigue Properties of type 316LN Stainless Steel in Air and Mercury, SNS-101060200-TD0001-R00, October 2002.